INTERNATIONAL SOCIETY FOR
SOIL MECHANICS AND
GEOTECHNICAL ENGINEERING

This paper was downloaded from the Online Library of the International Society for Soil Mechanics and Geotechnical Engineering (ISSMGE). The library is available here:

https://www.issmge.org/publications/online-library

This is an open-access database that archives thousands of papers published under the Auspices of the ISSMGE and maintained by the Innovation and Development Committee of ISSMGE.

Performance of geoysnthetic-reinforced flexible pavements: Numerical parametric study

Performance de geosynthetic renforces de chausses souples: Etude Paramétrique Numérique

B. Saad, H.S. Mitri & T. Hamade
McGill University, Montreal, Quebec, Canada

ABSTRACT
A finite element parametric study was conducted in this paper to explore the increase in the rutting and fatigue resistance brought about to a conventional pavement system due to the insertion of geosynthetic membrane under different foundation types and geosynthetic locations. The study concluded that regardless of the foundation quality the longest life against fatigue distress was achieved when the geosynthtic was placed at the bottom of the asphalt concert layer; whereas, the optimum location for prolonging the rutting life was found at the 1/3 of the base thickness from the bottom. However, the life extension against rutting in this case was dependent on the foundation quality. Further investigations are required to validate the conclusions obtained for pavements with different foundation and geosynthetic parameters as well as loading features.

RÉSUMÉ
Une étude paramétrique par les éléments finis a été effectuée afin d'examiner l'amélioration des résistances en orniérage et fatigue obtenues suite à l'installation d'une membrane géosynthétique localisée dans différentes positions pour différents types de fondations. L'étude a conclue que la vie la plus longue contre le phénomène de fatigue est obtenue quand la membrane géosynthétique est placée immédiatement en dessous de la couche d'asphalte, quelque soit la qualité de la fondation. L'emplacement optimal pour prolongée la vie contre l'orniérage se trouve à 1/3 de l'épaisseur de la base. Cependant, l'augmentation de la vie contre l'orniérage dans ce cas est dépendante de la qualité de la fondation. D'autres investigations sont requises afin de valider les conclusions déduites pour le pavement ayant un type différent de fondation et de géosynthétique, ainsi que les charges appliquées.

Keywords : pavements, geosynthetic, rutting, fatigue, numerical analyses

1 INTRODUCTION

The potential of the geosynthetic as a reinforcing material of pavements has been well recognized for almost three decades, Refer for example to Haas (1984), Miura et al. (1988), Barksdale et al. (1989), Ling and Liu (2001), Perkins and Cortez (2005) and Khodaii et al. (2008). However, the mechanism by which the geosynthetic operates under various characteristics of the pavement components and membrane has not been explored fully yet. Therefore, several pavement agencies and universities are currently motivated to conduct research work on geosynthetic and integrate it in the design methods of conventional pavements (CRREL 2003) so that significant cost is saved and thus efficient design is achieved. Herein, numerical analyses are carried out in the form of a parametric study to evaluate the benefits added to a conventional flexible pavement, which is composed of the three classic layers: subgrade, granular base, and asphalt concert (AC), as a consequence of using the geosynthetic membrane.

2 PARAMETRIC STUDY

Deciding the conditions under which the geosynthetic reinforcement is useful as a result of its utilization is dependent on the parameters of the pavement layers as well as the geosynthetic reinforcement and its location within the pavement system. Therefore, a finite element parametric study was conducted to investigate how the geosynthtic efficiency of improving the structural performance of a conventional flexible pavement would vary based on the quality of its foundation and the geosynthtic location within such foundation. In the study, three conventional pavement systems having the same AC layer but differed in their foundation as follows: weak base over clayey subgrade (system 1), strong base over clayey subgrade (system 2), and weak base over silty sand subgrade (system 3) were studied. In addition, three locations of the geosynthetic: at the bottom of the AC layer, at the bottom of granular base, and at the granular base lower third from the bottom, were examined for each system analyzed. The simulations were conducted with ADINA nonlinear finite element (FE) code (ADINA 2001) using the implicit dynamic method.

3 FINITE ELEMENT MODEL SET-UP

3.1 *Geometry, loading configuration, and boundary conditions*

In this paper the three-dimensional (3D) analysis was considered for simulating the geometry. In addition, a single wheel load of 40 kN (9000 pounds) with a tire contact pressure of 550 KPa (80 psi) and a rectangular contact domain with dimensions L= 406.4 mm (16 in) and B =177.8 mm (7 in), which were decided based on Yoder and Witczak (1975), were adopted. To reflect the effect of the wheel load passage, this loading rectangle was applied through a triangular wave with duration of 0.1 second corresponding to an average speed of around (32.18 km/hr) 20 mph (Barksdale 1971). As the load was applied at the center of the road and due the double symmetry of geometry and boundary conditions about the horizontal x and y axes only a quarter model was considered. This quarter model was 2.5 m wide, 3.0 m long, and 2.8 m deep (Figure 1).

3.2 *Materials constitutive response and associated parameters*

The materials of the systems analyzed were taken from literature to represent realistic pavement layers and geosynthetic reinforcement; refer to Table 1 for the constitutive

Proceedings of the 17th International Conference on Soil Mechanics and Geotechnical Engineering
M. Hamza et al. (Eds.)
© 2011 IOS Press
doi:10.3233/978-1-60750-031-5-3518

models used to model these layers with the respective mechanical parameters and the underlying sources from which these parameters were adopted.

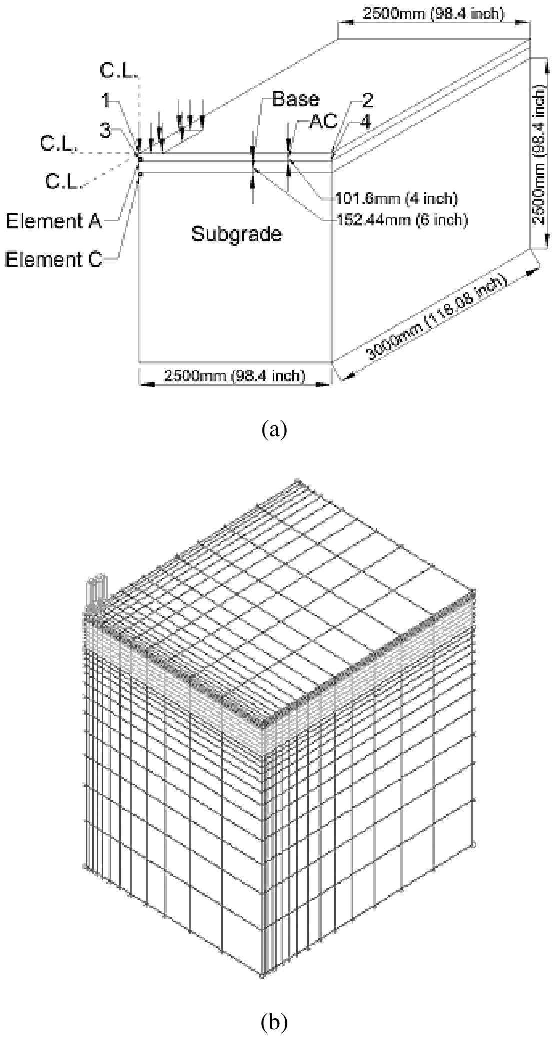

Figure 1. Constructed Model: (a) Geometry, (b) Mesh; system's response is reported at elements A and C with edges 1-2 and 3-4

3.3 *Model truncation*

The eight-node isoparametric element with reduced integration scheme was used to model the pavement layers and the isoparametric four-node membrane element was used to model the geosynthetic reinforcement. This membrane element allows only for in-plane stresses and does not take any bending nor compression stresses. Additionally, meshing the model was performed so that (a) the element aspect ratio remained close to one where the strain and stress gradients were high to achieve faster convergence in these areas, and (b) fine truncation was achieved near the loaded area to capture the steep stress and strain gradient in these areas. The AC, base, and subgrade were modeled with 720, 1080, and 2160 elements, respectively; see Figure 1 for the mesh constructed. Further, it was assumed that no slippage occurred between the material layers and thus no interface elements were used. The full bonding of the geosynthetic and the surrounding layers is an acceptable assumption for the case of a paved system where the allowed surface rutting of such system surface is small; refer for example to Barksdale (1989).

4 RESULTS AND DISCUSSIONS

The structural performance of the sections analyzed was evaluated by (i) the maximum horizontal strain transmitted to the bottom of the AC layer, ε_t^{max} , being found at element A (Figure 1), and (ii) the maximum vertical compressive strain transmitted to the bottom of the subgrade, ε_c^{max}, being found at element C (Figure 1), which criteria are commonly used to measure pavement fatigue and rutting, respectively. Refer to Table 2 for the magnitudes of ε_c^{max} and ε_t^{max} obtained. Additionally, the plots of the horizontal strain transmitted along the bottom edge of AC layer (edge 3-4 in Figure 1), and the vertical surface deflection (edge 1-2 in Figure 1) were reported at the peak load; refer to Figures 2 and 3 for the plots obtained.

4.1 *On the fatigue distress*

The results reported in Table 2 demonstrate that for all foundation types considered the geosynthetic placed at the bottom of the AC layer and at 1/3 of the base thickness shows remarkable decrease of ε_t^{max} with more reduction produced when the membrane is placed at the former location. This is most likely because the geosynthetic in this case will participate directly in absorbing the horizontal tensile strain, which would otherwise be carried by the AC alone. While the amount of the reduction changes negligibly with changing the foundation quality for a membrane placed at the bottom of the AC, it varies considerably when the membrane is placed at a height of 1/3 of the base thickness.

Table 1. Materials data of the pavement layers and geosynthetic with the corresponding constitutive laws adopted

Layer	Subgrade		Base		AC	Membrane
Model	Modified Cam Clay		Drucker-Prager		Elastic	Elastic
Quality	Clay (weak)	Silty sand (strong)	Weak	Strong	Average	Average
Data	E = 8280 kPa ν = 0.25 M = 1 Γ = 2.1 k = 0.026 λ = 0.147 OCR = 1 e_0 = 1.08	E = 50646 kPa ν = 0.28 M = 1.24 Γ = 1.347 k = 0.0024 λ = 0.014 OCR = 1 e_0 = 0.34	E = 96793 kPa ν = 0.3 Ø = 25° (*)	E = 414000 kPa ν = 0.3 Ø = 38°	E = 4134693 kPa ν = 0.3	E = 4230000 kPa ν = 0.35
Source	(Desai and Siriwardane, 1984)	(Desai and Siriwardane, 1984)	(Liu et al. 1998) (*) Assumed	(Zaghloul and White, 1993)	(Zaghloul and White, 1993)	(Erickson and Drescher, 2001)

Legend: E: modulus of elasticity, ν : Poisson ratio, M: inclination of the critical state line, λ: compression index, k : recompression index, Γ: the specific volume, OCR: over-consolidation ratio, e_0 : initial void ratio, Ø,: friction angle.

Table 2. Fatigue strain (ε_t^{max}) and rutting strain (ε_c^{max}) predicated for the pavement sections analyzed.

Pavement foundation	Geosynthetic location in base	(ε_t^{max}) x 10^{-4}	(ε_c^{max}) x 10^{-3}	(ε_t^{max}) Decrease (%)	(ε_c^{max}) Decrease (%)
Weak base over clayey subgrade	N/A	3.73	-3.88	-	-
	Bottom of base	3.61	-3.77	3.2	3
	Lower 1/3 of base	2.89	-2.93	22	24
	Top of base	1.93	-3.34	48	14
Strong base over clayey subgrade	N/A	3.21	-3.25	-	-
	Bottom of base	2.65	-2.76	17	15
	Lower 1/3 of base	2.14	-2.13	33	34
	Top of base	1.71	-2.88	46	11
Weak base over silty sand subgrade	N/A	3.46	-1.67	-	-
	Bottom of base	3.40	-1.64	2	2
	Lower 1/3 of base	2.86	-1.39	17	16
	Top of base	1.80	-1.45	47	13

Also, the results in Table 2 show that the decrease in ε_t^{max} obtained with the placement of geosynthetic at the 1/3 of the base thickness is more pronounced in case of the clayey subgrade, which is relatively much weaker than the sandy silt subgrade. In this case the reduction of ε_t^{max} achieved for a pavement with a stronger base is higher than the ε_t^{max} reduction produced for a pavement with a weak base. Furthermore, it is also observed upon examining the FE results that for all systems analyzed the geosynthetic gives higher ε_t^{max} reduction in the areas where large stresses existed; i.e., in the vicinity of the wheel load application zone, with the maximum reduction being achieved at the node having the maximum horizontal tensile strain. As a demonstration of this observation the plot of the horizontal strain transmitted along the bottom edge of AC is shown for the system having weak base over clayey subgrade; refer to Figure 2. The response of other systems is not shown herein due to the space constrain. On the other hand, geosynthetic placed at the bottom of the base does not lead to a material benefit except in the pavement system having a strong base and clayey subgrade where almost 15 % decrease of ε_t^{max} is observed.

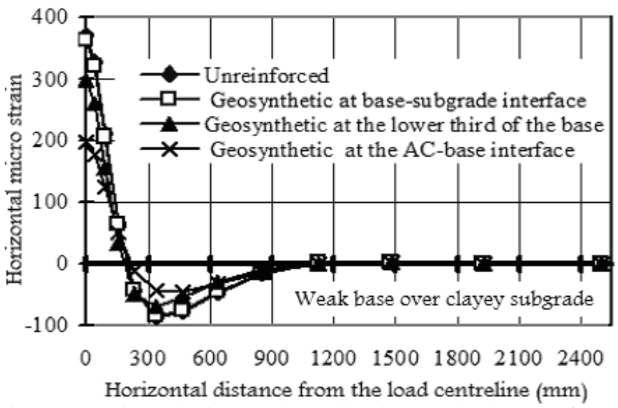

Figure 2. Horizontal micro strain predicted along the bottom of AC layer [(edge (3-4) in Figure 1] considered at the peak load.

4.2 *On the rutting distress*

Among the three locations examined, Table 2 shows that at 1/3 of the base thickness from the bottom is the most beneficial location for reducing ε_c^{max}. Such reduction is more pronounced when the subgrade is weak. In this case the section having strong base experiences a decline of 34 % in ε_c^{max} which is almost double the decline of 16 % achieved for the section with the weak base. However, for both the weak and strong subgrades, the decrease of ε_c^{max} due to placing the membrane at the bottom of the base seems to be insignificant unless the base is strong. Moreover, the results in Table 2 suggest that placing the membrane at the top of the base will lead to a considerable drop in ε_c^{max} reaching to 14 % . Such drop changes very slightly with the change of the quality of the base and subgrade.

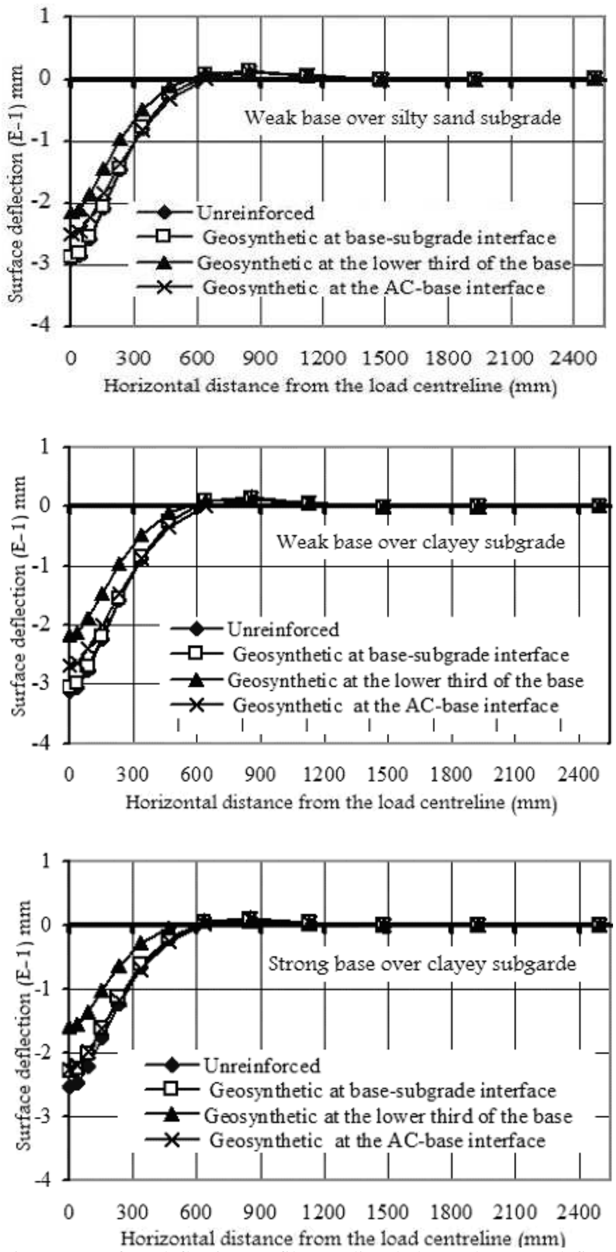

Figure 3. Surface deflection profiles predicted along edge (1-2) defined in Figure 1 considered at the peak load for the three foundation types analyzed.

Further, Figure 3 shows that the reduction in the surface deflection always reaches its peak immediately under the wheel load center implying that the increase in the pavement system stiffness brought about by the membrane reaches its maximum at this location (reduction in surface deflection reaches to 35% at this location). However, it is shown in this figure that the difference in the surface deflection (taken as an absolute value) between the reinforced systems and unreinforced systems tends to decrease by moving along the edge away from the load center until it disappears completely at a distance of 1100 mm from the wheel load centre.

5 RESULTS ASSESSMENT IN LIGHT OF LITERATURE

The following remarks could be made upon comparing the results obtained from this study with the results of some major relevant investigations reported previously in literature: (i) it was found in this study that the reinforcement effect was more pronounced for a weaker subgrade. This finding is in agreement with the conclusions reported by Barksdale et al. (1989) and Ling and Liu (2003), (ii) under the relatively moderate load and thin base considered, the results demonstrated that the geosynthetic remarkably improved the pavement structural performance. This result is consistent with the findings of Berg et al. (2000), (iii) the 15 to 20 % reduction of ε_c^{max} reported by Dondi (1994) due to placing the membrane at the bottom of strong base overlying clayey subgrade agreed well with the corresponding ε_c^{max} reduction amount obtained from the current investigation which was 15 %. However, Dondi (1994) showed that remarkable reduction of ε_t^{max} reaching to 20% was resulted after placing the membrane at the bottom of a strong base underlain by a clayey subgrade. Whereas, the corresponding reduction obtained in the current study did not exceed 4%, (iv) the ε_t^{max} decline of 30 % reported by Haas (1984) when placing the membrane at the bottom of the AC was less than the ε_t^{max} decline obtained in this study which ranged between 46 to 48 %. As could be seen from the above comparisons, there were little discrepancies between some of the observations reported in this study and the corresponding conclusions of some of the investigations existing in literature. These discrepancies can mainly be attributed to the difference between the pavements and geosythetic parameters adopted herein and those considered by such investigations. However, further investigations are required to confirm this statement.

6 CONCLUSIONS

A finite element parametric study was conducted to explore the increase in the rutting and fatigue resistance brought about to a conventional pavement system due to the insertion of geosynthetic membrane under different foundation types and locations of the geosynthetic. The study concluded that, for the three geosynthetic locations examined (at the bottom of AC, at the bottom of base, and at lower third of the base), the optimum location of the geosynthetic for prolonging the pavement fatigue life was at the bottom of the AC layer. The fatigue strain reduction, which reached 48 % in this case, seemed to change immaterially with the foundation quality. However, the best location for reducing the pavement rutting was found to be at a third of the base thickness, which resulted in rutting strain reduction reaching 34 % when the subgrade was weak and the base was strong. In general, good agreement between the observations drawn from this study with those reported in the relevant literature was found. Further future field and/or laboratory investigations are recommended to confirm the validity of the conclusions obtained and to inspect their value for pavements with layers, geosynthetic, and loading features different from those considered in this work.

REFERENCES

ADINA. 2001. Finite Element Computer Program, Theory and Modeling Guide, ADINA R&D Inc., Watertown, MA, Volume 1, Report ARD 01-7.

Barksdale, R.D. 1971. Compressive Stress Pulse Times in Flexible Pavements For Use in Dynamic Testing, Highway Research Record 345, Highway Research Record: 32-44.

Barksdale, R.D., Brown, S.F. and Chan, F. 1989. Aggregate Base Reinforcement of Surfaced Pavement, Geotextiles and Geomembranes, 8: 165-189.

Berg, R.R., Christopher, B.R. and Perkins, S.W. 2000. Geosynthetic Reinforcement of the Aggregate Base Course of Flexible Pavement Structures, GMA White Paper II, Geosynthetic Materials Association.

Cold Regions Research and Engineering Laboratory (CRREL). 2003. Base-Course Reinforcement: Proposed FHWA Pooled Fund Study, FHWA Project TPF-5 (010), USACE Engineer Research and Development Centre.

Desai, C.S. and Siriwardane, H.J. 1984. Constitutive Laws For Engineering Material, Prentice-Hall, Inc., Englewood Cliffs, NJ.

Dondi, G. 1994. Three- dimensional Finite Element Analysis of a Reinforced Paved Road, In Fifth International Conference on Geotextiles, Geomembranes and Related Products, Vol.1, Singapore, 95-100.

Erickson, H. and Drescher, A. 2001. The Use of Geosynthetics to Reinforce Low Volume Roads : Final Report, Minnesota Department of Transportation, Minnesota, Report No MN/RC-2001-15.

Haas, R. 1984. Structural Behavior of Tensar Reinforced Pavement and Some Field Applications, In Proceeding of Polymer Grid Reinforcement Conference, Thomas Telford, London, 166-170.

Khodaii, A., Fallah, S. and Nejad, F.M. 2008. Effects of Geosynthetic on Reduction of Reflection Cracking in Asphalt Overlays, Geotextiles and Geomembranes, 27(1): 1-8.

Ling, H. I. and Liu, Z. 2001. Performance of Geosynthetic-Reinforced Asphalt Pavements, Journal of Geotechnical and Geoenvironmental Engineering, 127(2):177-184.

Ling, H.I. and Liu, H. 2003. Finite Element Studies of Asphalt Concrete Pavement Reinforced with Geogrid, Journal of Engineering Mechanics, 129(7): 801-811.

Liu, X., Scarbas, A., Blaauwendraad, J. and Genske, D.D. 1998. Geogrid Reinforcing of Recycled Aggregate Materials for Road Construction: Finite Element Investigation, Transportation Research Record 1611, TRB, National Research Council, Washington, D.C.,78-85.

Miura, N., Sakai, A., Taesiri, Y., Mouri, K. and Ohtsubo, M. 1988. Model and Field Tests of Reinforced Pavement on Soft Clay Ground, International Geotechnical Symposium on Theory and Practice of Earth Reinforcement, Vol.2, Fukuoka, Japan, pp.227-232

Perkins, S.W. and Cortez, E.R. 2005. Evaluation of Base-Reinforced Pavements Using a Heavy Vehicle Simulator, Geosynthetic International, 12(2): 86-98

Yoder, E.J. and Witczak, M.W. 1975. Principles of Pavement Design, Second Edition, John Wiley & Sons Inc.

Zaghloul, S.M. and White, T.D. 1993. Use of a Three-Dimensional Dynamic Finite Element Program for Analysis of Flexible Pavement, Transportation Research Record 1388, TRB, National Research Council, Washington, D.C., 60-69.